EROSION AND CORROSION BY MICRO-JETS AND HIGH TEMPERATURE CAVITY IMPACTION ON METAL SURFACES

Gil Bazanini gil.bazanini@udesc.br[1]
Auzany Freitas Barbosa Jr.[1] **g-calc@bol.com.br**
Nicodemus Neto da Costa Lima[1] **nicodemus.lima@udesc.br**

[1] Universidade do Estado de Santa Catarina; Rua Paulo Malschitzki, 200 - Campus Universitário Prof. Avelino Marcante - Bairro Zona Industrial Norte - Joinville - SC - Brasil CEP: 89.219-710 - Fone:(47) 3481-7900.
Universidadenstitution and address for third author

Abstract. *Present work examines material surface damage by cavitation erosion of metals or the wear phenomenon owing to water bubbles collapse near the metallic surface. Material surface damage by cavitation erosion is due to wear mechanisms of hot liquid micro-jets impingement and impaction. To explain these erosion mechanisms based on water flow and mechanical properties of tested materials, experimental cavitation in tap water was investigated, using acompact rotating disk equipment. In this rig, a rotating disk with cavitation inducers and specimens fixed on it run in tap water to provide cavitating flow similar to service conditions in pumps and propellers. Cast iron, carbon steel and bronze specimens were tested in this test rig. The cavitation damage mechanisms were observed by scanning electron microscope after each 5 hours working under cavitating conditions. The specimens surfaces were worn out by cavitation erosion mechanisms, resulting in pitting formation or mass loss. All specimens presented surface damage. Pit diameter size was about to 50 μm. Calculations of the temperature of the cavity contents in its final stage of the collapse resulted in great value for the temperature (of about 2,500 K) of the vapor and gas trapped inside it. The damages on the specimens are analyzed showing pits and approximate circular regions on their surfaces. An explanation is presented here based in temperature calculations and images of the specimens after the collapses. The pits are made by liquid micro-jets impingement while its surrounding approximate circular regions, showing some aspect of heating and craters are credited to the high temperature impaction of the bubble contents in the final stages of its collapse. The influence of heat by conduction rejected by the cavity is also studied here. Materials analyzed are commonly used in manufacturing of rotors of feed-water pumps.*

Keywords*: Damage, Erosion, Metal.*

1. INTRODUCTION

Damage by cavitation is a complex phenomenon that includes hydrodynamic, mechanical, metallurgical and chemical processes (Berchiche et al, 2000). Here, the phenomenon was tested in 1020 carbon steel, and bronze, as well as for cast iron specimens. The cavitation phenomenon, the formation, growth and collapse of air and vapor bubbles in liquids is, as well known, responsible for damage in metallic and non-metallic solid structures and equipments in liquid mediums, remarkably in water. The bubbles, also named cavities, nucleate from micro-bubbles of air present in the liquid medium. Such bubble formation phenomenon is named “cavitation inception” (Hammitt, 1980). The growth process involves primarily the action of pressure forces, and these are the results of the interplay of surface action, inertia and viscosity (Bazanini and Hoays, 2008). In most simple terms, it is the balance of the static force at the bubble wall between the surface tension and pressure differences caused by physical properties.

The most usual example is the cavitation erosion in centrifugal pumps (Hattori and Kishimoto, 2008). Liquid micro-jets impingement, passing through bubbles close to a solid surface, cause surface damages such as plastic deformation and material loss. These micro-jets are caused by the presence of the bubble when collapsing near a solid surface, and influenced by the proximity to this surface (Figure 1). The micro-jets and bubble final impaction against the solid surface are responsible for material loss from the surface or plastic deformation.

To a better understanding of the phenomena, that is the effects of cavitation on solid surfaces, several rigs have been developed along the last decades, such as the jet-impact damage rig consisting of water liquid jets impinging in specimens fixed on rotating disks. To reduce the time of the experiments, it was designed the vibratory apparatus where the specimens are set to vibrate in the test liquid. There is the vertical (referring to the rig axis) rotating disk (Cheng et al., 2013), where a disk with the specimens fixed on its surface is rotating in water to provide the cavitating flow, and finally (perhaps important in the sense that reproduces reasonable well the phenomenon of the flow through a centrifugal pump), the horizontal rotating disk rig (Rao et al., 1980; Vivekananda, 1983; Zhiye, 1983).

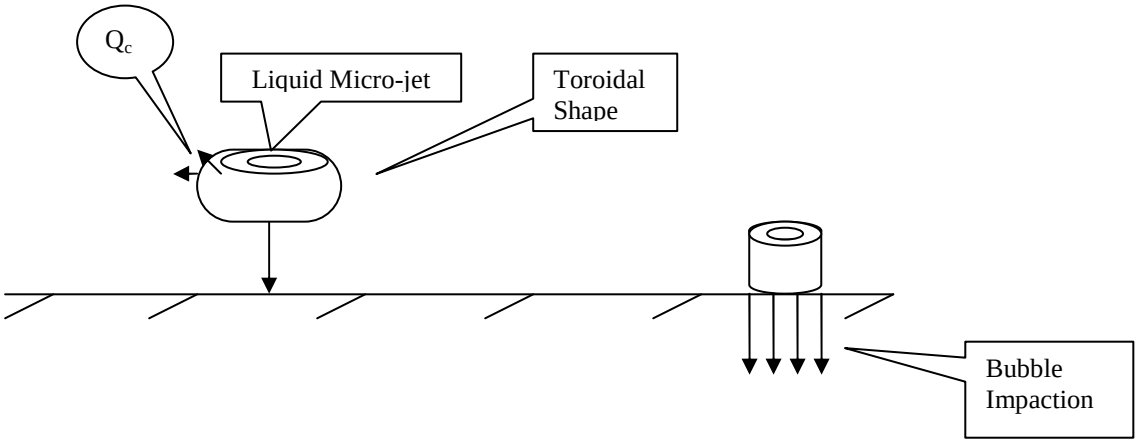

Figure 1. Bubble collapse and impaction against a solid surface.

2. TEST RIG

The test rig proposed by Bazanini and Bressan (2007) consists of a water chamber inside which a metallic disk rotates. On the disk surface there are cavity inducers (through-holes) close to the specimens. The disk is fixed on the rotating shaft and can be removed to attach the specimens. A glass cover is mounted on the chamber to visualize the flow and bubble formation inside it (see Figure 2).

The purpose of the rig is to create cavitation bubbles similar to service conditions in rotor pumps and propellers. The bubbles generated by the bubble inducers will be responsible for the cavitation erosion and deformation of the specimens fixed on the disk surface.

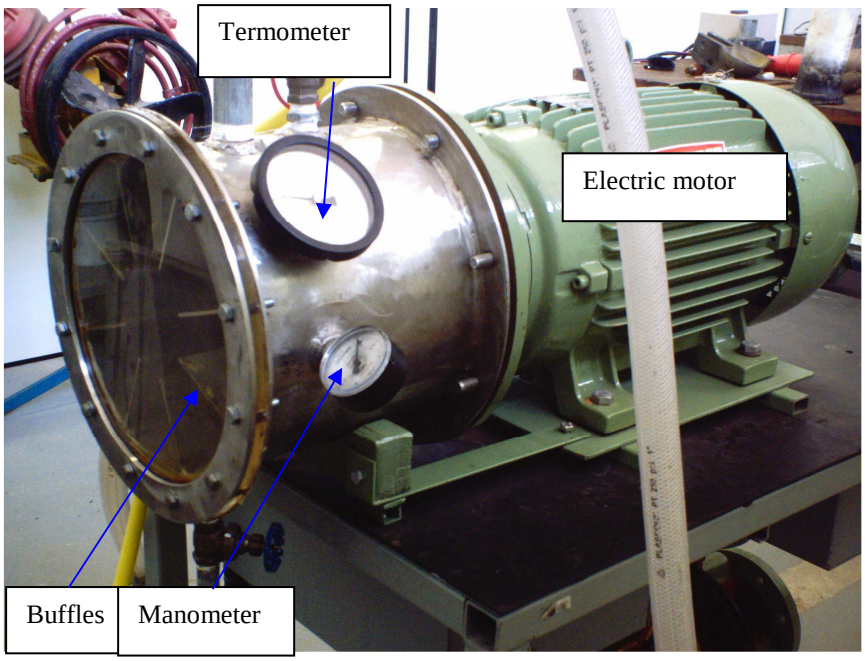

Figure 2. Some details of the test rig.

For cooling purposes and constant fresh tap water supplying, a water reservoir was used to circulate the water inside the chamber. Inlet and outlet piping are provided by control valves and a filter to protect the pump from small particles resulting from the erosion process.

Using the “intermediary casing”, commonly used to connect pumps to electric motors, it was possible to avoid the use of bearing and coupling components, resulting in a shorter shaft and a compact disk rig. The chamber now replaces the pump, improving the experiments which are performed in a more realistic condition. The rig was operated at 4400 rpm (resulting in a water flow average peripheral velocity at the specimen surface of 47.9 m/s during 5 to 15 hours to

obtain the results presented here. The experiments were performed at atmospheric pressure and the water temperature in the chamber was kept constant at 39°C by fresh tap water flow circulation.

In the present work, bronze, 1020 carbon steel, bronze and cast iron were used as test specimens. To fix the disk to the to electric motor shaft, a flange was specially manufactured in bronze.

The cooling water used was of 8.8 liters per minute.

Initially, the test specimens used in these experiments had their chemical compositions determined by mass spectometer analysis. The specimen chemical compositions are listed in Table 1. In addition, Vickers micro-hardness (mHV) of some test specimens were also obtained before testing.

Table 1. Chemical composition and Vickers micro-hardness of test specimens.

Chemical element (% wt)	C	Mn	Ni	Fe	P	Cu	Mg	Si	Sn	Zn	Pb	Al	Vickers micro-hardness (HV300gf)
Cast iron	3.797	0.044	0.084	93.000	0.049	0.484	0.026	2.516	-	-	-	-	240.1
Bronze	-	-	0.191	0.089	0.012	76.134	-	0.005	3.066	5.603	14.900	-	88.0
Carbon Steel	0.219	0.683	-	98.598	-	0.043	-	0.225	0.0088	-	-	0.0141	180.0

The behavior of each material will be discussed later, although bronze specimens are expected to be more susceptible to erosion by cavitation (Bazanini and Bressan, 2007). After each 5 hours in cavitating conditions, the test specimens are cleaned by ultrasound and dried. Also, images of the specimens were obtained using a scanning electron microscope (SEM).

3. MATHEMATICAL MODEL FOR THE BUBBLE TEMPERATURE CALCULATIONS

In the equations of bubble temperature calculations, it is usually took into account the initial gas pressure P_{g0} (Pa), the initial vapor pressure P_{v0} (Pa), the adiabatic constants of the gas and vapor, K_g and K_v., and the cavity initial radius R_0 (m). T_0 is the cavity (or bubble) internal initial temperature (K).

For the gas and the vapor trapped inside the bubble, it is also considered the effect of the van der Waals hard core radii a_g (m) and a_v (m), (Barber et al., 1997). In fact, gas and vapor are being considered to obey the van der Waals equation of state for real gases. This is important because of the raising pressures within the bubble during the collapse.

$$T = \frac{T_0}{\left(P_{v_0} + P_{g_0}\right)}\left[\frac{P_{g_0}\, R_0^{\,3(k_g-1)}}{\left(R^3 - a_g^3\right)^{(k_g-1)}} + \frac{P_{v_0}\, R_0^{\,3(k_v-1)}}{\left(R^3 - a_v^3\right)^{(k_v-1)}}\right] \tag{1}$$

Using Equation (1), the temperature as a function of the radius was calculated (Bazanini et al., 2016), reaching a maximum value of about 2,500 K for the bubble contents, in its final stages of collapse for a bubble of an average size (radius of 1mm, for example). Anyway, there are always such high temperature values in that compression.

It is known that heat conduction in fluids may occur when they are in direct contact at different temperatures (Landau and Lifshitz, 1959). In this case, there is heat conduction from the bubble to the surrounding liquid.

Making the energy balance for the bubble, we must equalize the heat transfer with the work and the bubble energy (the first law of thermodynamics):

$$3k\frac{dT}{dR}4\pi R^2 = PdV + \frac{4}{3}\pi\left(R_0^3 - R^3\right)dP \tag{2}$$

Where k is the conduction heat transfer coefficient (for the liquid water, W/m.k), P is the bubble pressure (Pa) and V is the bubble volume (m^3). The last term of the second member of equation (2) appears as the bubble energy term in Muller at al. (2012) and Frank and Michell (2005). That will result an Equation to estimate the temperature that must be reduced (for convection) from the bubble contents temperature by compression:

$$\Delta T = -\frac{\frac{P_\infty R_0^3}{3}\left(\frac{1}{R_0}-\frac{1}{R}\right)+\frac{P_\infty}{6}\left(R_0^2-R^2\right)}{3k} \tag{3}$$

That temperature reduction can act as a “cooling effect” of the bubble contents due to this heat conduction from the bubble to the surrounding liquid.

As the collapse proceeds, the temperature increases due to the compression of the mixture vapor-air. Since the collapse phenomenon is too fast (of about miliseconds), the question is if there is enough time for conduction heat transfer from the bubble to the surrounding liquid to reduce substantially the increase of the bubble internal temperature. The results can be seen on Table 3, where the temperature reduction (“cooling effect”) was calculated for two regular bubble radii. It agrees with the fact that how greater is the radius, greater is the heat transfer area.

4. RESULTS

The calculated results obtained from the solution of Equation (3) are listed in table 2 below. It is possible to see that the “cooling effect” of the bubble contents due to heat conduction from the bubble to the surrounding liquid is negligible, when compared with its final temperature of 2,500 K, leading to raising energy in the bubble contents. That energy will be released against the close boundaries later.

Table 2. Calculated temperature reduction by conduction heat transfer during the bubble collapse.

Bubble initial radius (mm)	3.5	1.0
ΔT by conduction heat transfer (K)	**15**	**1**

Analyzing actual bubble collapse photographs, it is possible to see that, at the final moment of collapse, the bubble usually moves toward the close solid surface (Brennen, 1995).

The cavities collapsing near the specimen surfaces, led to some cavitation damage (not necessarily with mass loss; Cheng et al., 2013), basically by micro-jets impingement formed during the collapse, and hot bubble impaction against the solid surface at the end of the collapse, added by pressure waves in the case of bubble oscillations. After 5 hours of tests, it is already possible to see the damages caused by cavitation on the specimens. Images of the specimens were observed by the scanning electron microscope (SEM). A magnification of 200 times was used in Figure 3 for the cast iron specimen. It is possible to see the “pits” and a process of surface oxidation after 10 hours of tests.

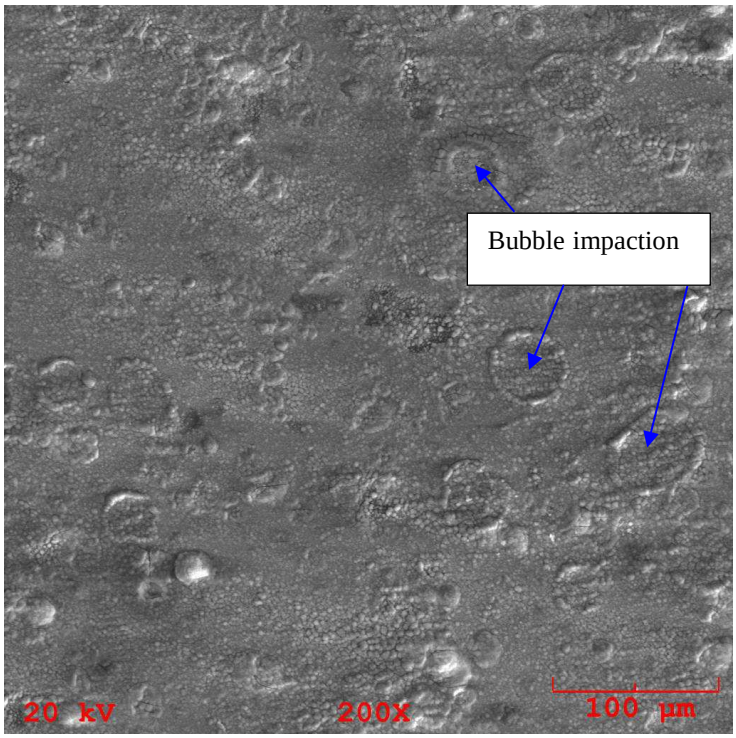

Figure 3. Cast iron specimen in oxidation process after 10 hours of tests with magnification of 200 x.

Some craters (with burned aspect) with surface oxidation could be seen for the cast iron and the carbon steel specimens (Figures 3 and 4, respectively).

For the bronze specimen, a high level of erosion was detected (Figure 5), leading to mass loss by erosion but no crater areas was observed, possibly due to its fast erosion rate. For the cast iron and the carbon steel test specimens a mass formed by oxidation (as expected) of the specimen surface was formed in the surface.

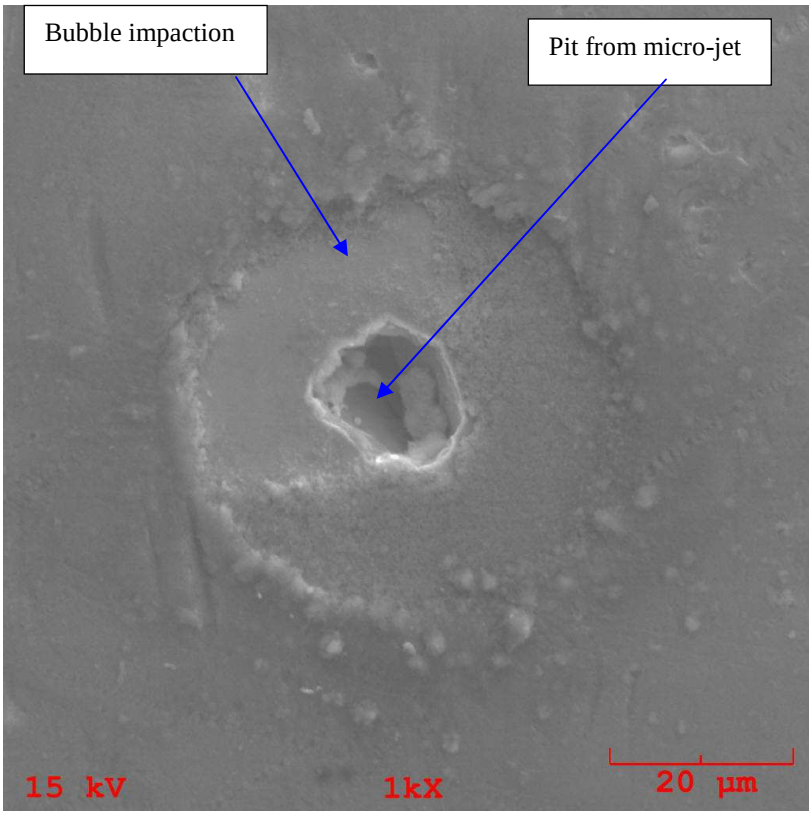

Figure 4. Carbon steel after 5 hours of tests with magnification of 1000 x.

Those craters seen in the images of Figures 3 and 4, after 10 hours of operation rig for cast iron, and 5 hours for the carbon steel specimens, with magnification of 200x and 1000x, respectively, were caused by cavitation micro-jets impingement and hot bubble impaction in the final moments of the bubble collapse.

The erosion rate on the surface of the bronze specimen, after 10 hours submitted to cavitating test conditions, is clearly seen in Figure 5 for a magnification of 100 x.

Figure 6 shows the mass loss as a function of time for the bronze specimen. The mass loss is approximate constant, since there is no mass gain by surface oxidation for the bronze.

The temperatures inside de bubble, as calculated by Equation (1), may reach 2,500 K for an average bubble, of about of 1 mm in initial diameter, for example (Bazanini et al., 2016).

For the cast iron and the carbon steel test specimens, the detected mass loss by cavitation erosion is constant after a while, because there were two mechanisms involved: one was the mass loss of the specimen by cavitation erosion and the other was the mass gained by oxidation of the specimen surface. So, it was not possible to observe the mass loss properly by cavitation for those materials.

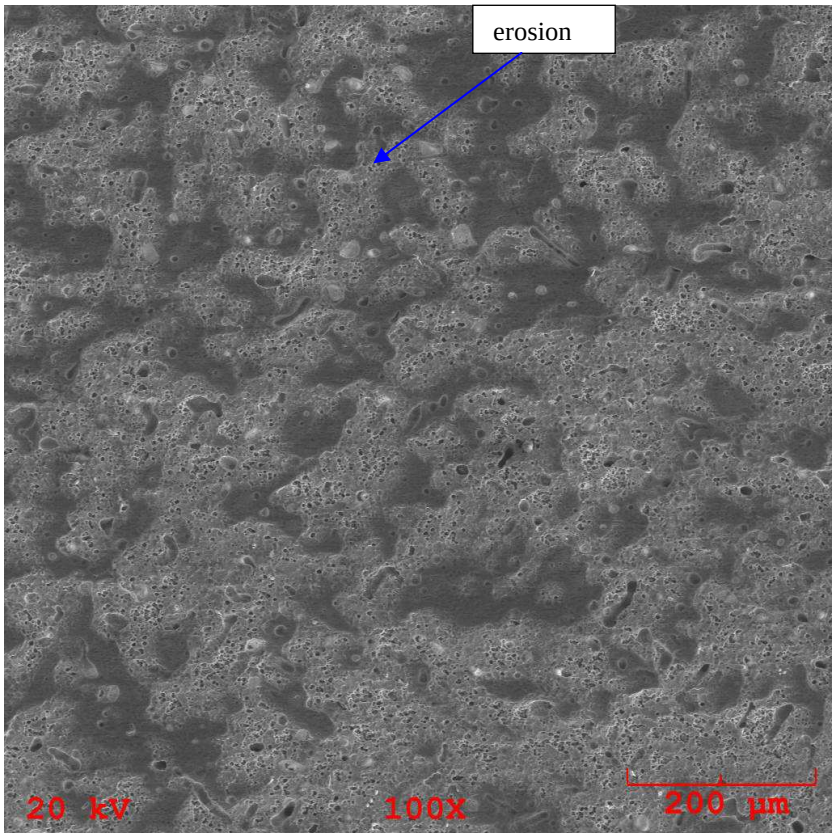

Figure 5. Bronze test specimen after 10 hours in cavitant conditions with magnification of 100 x.

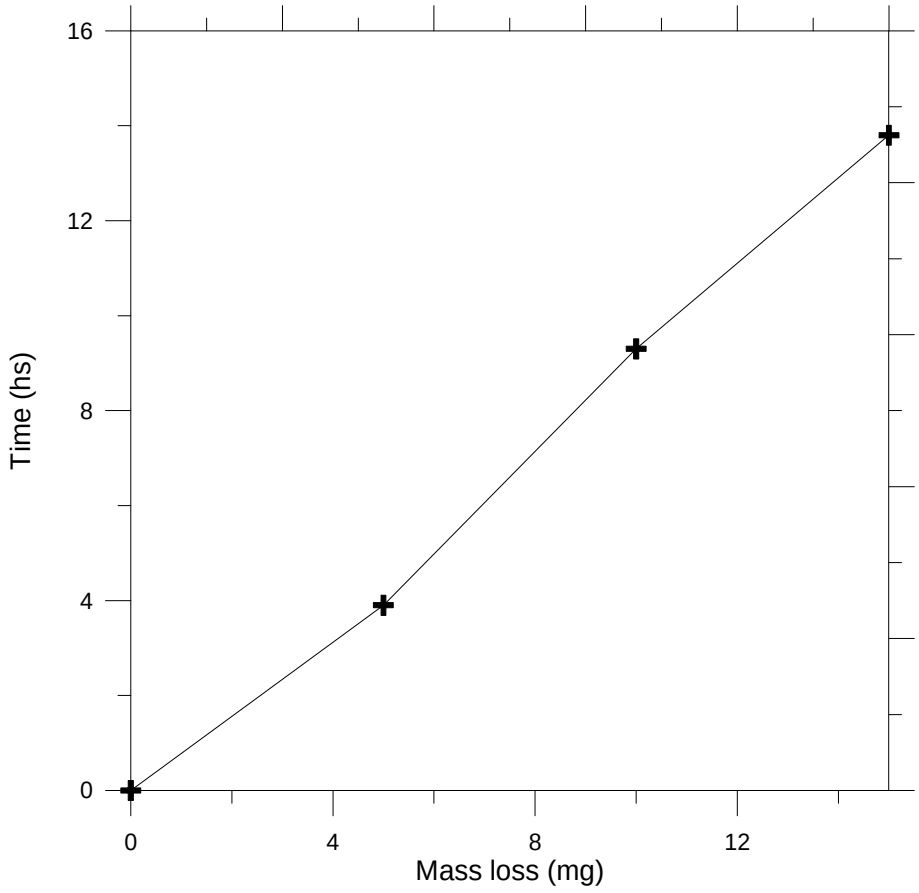

Figure 6. Mass loss curve for bronze test specimen after 15 hours in cavitant conditions.

5 CONCLUSIONS

All specimens presented some surface damage: worn pits formation, or mass loss resulting from cavitation erosion. The bubble inducer caused the expected cavitation effects on the tested metal specimen surfaces.

Craters are always formed around the cavitation pits. They are formed by liquid microjets associated to high temperature impaction of the bubble contents on the final stages of the collapse process.

For the cast iron and the carbon steel test specimens it was not possible to measure the mass loss by cavitation properly, since, if there was mass loss of the specimen by cavitation erosion, there was also a mass gained by oxidation of the specimen surface, what led to a constant approximate value after some hours in cavitating conditions. So, these two materials tested showed similar behaviors under cavitating conditions.

Anyway, some pits and crater areas could be seen for the cast iron and the carbon steel specimens, although already with some oxidation of the specimen surface.

The “cooling effect” of the bubble contents due to heat conduction from the bubble to the surrounding liquid is negligible, that is, such heat conduction does not affect considerably the bubble energy gained by the compression process. This accumulated energy will be released against the close solid surface on the final stages of the bubble collapse, leading to craters, pits and mass losses.

No craters were seen in the bronze specimens, certainly due to its high level of erosion observed. The expected craters formed are removed by the continuous erosion process.

The more elucidative, although qualitative, conclusion of these experiments was that the craters are “individual” marks, almost like an identification of each bubble, instead of the elderly belief of initial damage by fatigue failure. The fatigue may occur just in an ultimate phase of the process, when these craters are already superposed to each other.

6 ACKNOWLEDGMENTS

The authors would like to gratefully thank the financial support received from FAPESC (Foundation for Research Support of the Santa Catarina State).

7. REFERENCES

Barber, B.P., Hiller R.A., Löfstedt R., Putterman S.J. and Weninger K.R., 1997, “Defining the Unknowns of Sonoluminescence”, Physics Reports, Vol. 281, No. 2, pp. 65-143.

Bazanini G., Bressan J.D., Lima N.N.C. 2016, “Burned Areas in Metallic Specimens During Cavitation Erosion Tests”.Brazilian Archives of Biology and Technology v. 59.

Bazanini G., Bressan J.D., 2007, “Preliminary Experience With a New Compact Disk Apparatus for Cavitation Erosion Studies”. Wear, v. 263, p. 251-257.

Bazanini G., Hoays H.S., 2008, “Oscilações de Cavidades na Forma Adimensionalizada”. Primeiro Encontro Brasileiro Sobre Ebulição, Condensação e Escoamento Multifásico Líquido-Gás, Florianópolis, 28-29 de abril.

Berchiche N. Franc J.P.,Michel J.M.. 2000, “Un Modèle de Prédiction de L´Érosion dês Matériaux Ductiles par La Cavitation”. Mécanique dês Fluides. Academie des Scienses. Éditions Scientifique et Médicales. Elsevier.

Brennen C.E. 1995. “Cavitation and Bubble Dynamics”. Oxford University Press.

Cheng F. Jiang S., Liang J. 2013, “Cavitation erosion resistance of micro-arc oxidation coating on aluminium alloy”,Applied Surface Science 280 287– 296.

Frank,J.C..MichelL, J. P., 2005 ”Fundamentals of Cavitation”. Kluwer Academic Publishers, Dordrecht.

Hammitt F.G., 1980. “Cavitation and Multiphase Flow Phenomena”, McGraw-Hill Book Company.

Hattori S, Kishimoto M.. 2008, “Prediction of Cavitation Erosion on Stainless Steel in Centrifugal Pumps”, Wear , 265, 1870-1874.

Landau L D., Lifshitz E.M. 1959, “Course of Theoretical Physics, vol. 6. Fluid Mechanics”. Pergamon Press.

Muller M, A. S., Zima P.,Unger,J. 2012, “Energy Dissipated During the Cavitation Bubble Collapse Close to a Solid Wall”.Proceedings of the Eighth International Symposium on Cavitation, Singapore.

Rao P.V. , Rao B.C.S., Rao N.S.L., 1980, “Erosion and Cavity Characteristics in Rotating Components”. Journal of Testing and Evaluation. American Society of Testing and Materials, p. 127-142.

Vivekananda P. 1983, “Mechanism of Cavitation Damage Influence of Stacking Fault Energy on Erosion and Erosion Resistance of Steels and Coatings”. Ph.D. Thesis, Dept. of Civil Engineering, Indian Institute of Science, Bangalore, India.

Zhiye J., 1983, “An Experimental Investigation on Cavitation Erosion for Propeller Alloys”, China Ship Scientific Research Center Report, China.

8. RESPONSIBILITY NOTICE

The authors are the only responsible for the printed material included in this paper.